CP-SAR UAV DEVELOPMENT

P. Rizki Akbar , J.T. Sri Sumantyo , H. Kuze

Center for Environmental Remote Sensing (CEReS), Chiba University, Chiba 263-8522, Japan
- prilando_r_a@graduate.chiba-u.jp, (jtetukoss, hkuze)@faculty.chiba-u.jp

KEY WORDS: Axial Ratio, Circular Polarization, CP-SAR Sensor, UAV Platform, Parameters

ABSTRACT:

Up till now, only linearly polarized microwave radiation are employed by the Synthetic Aperture Radar (SAR) systems onboard spaceborne platforms. In general, such linearly polarized SAR (LP-SAR) systems are very sensitive to Faraday rotation in the ionosphere and platform posture, both of which will contribute to system noise superposed on the resulting backscattering signature. So as to improve the situation, currently a novel Circularly Polarized Synthetic Aperture Radar (CP-SAR) sensor is developed in our Microwave Remote Sensing Laboratory, Chiba University. As an early stage of the development of this CP-SAR sensor, we will make use of an Unmanned Aerial Vehicle (UAV) platform, called as Josaphat Laboratory Experimental UAV (JX-1) for testing CP-SAR capabilities. In this paper, we describe the CP-SAR hardware system design and CP-SAR parameters calculation with its results. The possibility of implementing a smaller antenna using the new CP-SAR technique than with conventional LP-SAR systems is shown. This research will contribute to the realization of a compact CP-SAR sensor, which can be installed on a small and low cost platform yielding a high accuracy SAR image data. The experience and knowledge of CP-SAR UAV experimental will be very valuable to realize a CP-SAR sensor onboard a small satellite platform as the final stage of the CP-SAR sensor development roadmap.

1. INTRODUCTION

Along its propagation in the ionosphere, the microwave signal vector will be distorted by Faraday rotation, as has happened in the current existing LP-SAR spaceborne system (Rignot, 2000). In comparison with the transmitted microwave signal, in downward direction, the incoming signal on the targeted surface will be altered in the signal plane orientation (Dubois-Fernandez et.al, 2008 and Wright et al., 2003), here, defined as tilt angle or τ. On the other hand, in the upward direction, the receiver system could suffer from mismatch polarization loss between the reflected linear polarization wave and the implemented LP-SAR antenna. As an example for L-band frequency which is suitable for land observation that covered by vegetation, the worst prediction of 40° rotation is described in Freeman (2003) and the value exceeding 25° can be found in the PALSAR sensor onboard the ADEOS-II satellite (Meyer and Nicoll, 2008). Since the microwave polarization plane will be determined by such Faraday rotation, the result of scattering mechanism will be different from time to time depends on the condition of the ionosphere. Hence, utilizing circularly polarized (CP) wave is expected to become a suitable solution for SAR spaceborne multitemporal observation (Dubois-Fernandez et al., 2008), as the incoming microwave signal plane orientation which hits the surface will stay the same with the transmitted one.

The circular polarized microwave has been widely use in the space communication system (ITU, 2002) and radio astronomy purposes (Raney, 2007) but it usage in SAR spaceborne for Earth observation has never been accomplished. Providing an antenna system which has sufficient value in circular polarization axial ratio, input impedance, S parameter and gain within a specific bandwidth around the frequency operational might have become the challenge. Hence, a novel SAR sensor based on circular polarization is currently under development in our Laboratory (Rizki Akbar et al., 2010). Here, a direct feeding antenna system is employed in our CP-SAR system (Baharuddin, 2009 and 2010). In the initial state of its development, CP-SAR sensor onboard an airborne platform named as Josaphat Laboratory Experimental UAV (JX-1) (see figure 1 and table 1), will be experimented using L-band (1.27 GHz) as the operational frequency. In the next section of this paper brief theory of microwave polarization, current LP-SAR system and the novel CP-SAR system will be discussed. Then, in section 3, UAV-CP SAR sensor hardware design, UAV-CP SAR parameter design will be described. The recent research results on UAV CP-SAR parameters and the conclusion will be

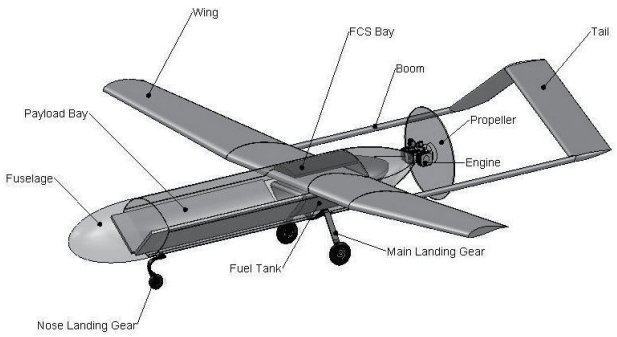

Figure 1. Josaphat Laboratory Experimental UAV (JX-1)

Payload	25 kg
Endurance	4-6 hours
Altitude	1-4 km
Speed	100-120 kph
Operating Mode	Remote Piloted Vehicle (RPV) non Autonomous Mode

Table 1. JX-1 Basic Specification

summarized in section 4 and 5. This UAV CP-SAR experiment will become a remarkable milestone in realizing CP-SAR system onboard a small satellite, which is scheduled to be launched in the year of 2014 (Sri Sumantyo et al., 2009).

2. THEORY

2.1 Microwave Polarization

The polarization of an electromagnetic wave can be categorized by using axial ratio (AR) parameter. From figure 2, the AR is defined as (Stutzman, 1993)

$$\varepsilon = cot^{-1}(-R) \tag{1}$$

where ε = ellipicty angle ($-45° \le \varepsilon \le 45°$)
R = the value of AR

The R is equal to 1 for perfect circular polarization and infinite for linear polarization. In the between of 1 and infinite, electromagnetic wave is classified as elliptical polarization. The absolute value of R is calculated as the ratio of the maximum (OM) and minimum value (ON) of electric field amplitude. In term of polarization sense, the sign of R is positive for right-handed (RH) polarization and negative for left-handed polarization (LH). The R parameter is also commonly stated in dB unit as 20 log|R|.

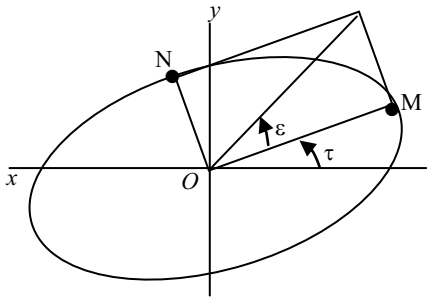

Figure 2. Electromagnetic Wave Polarization Parameters

In the antenna implementation, circular polarization can be generated by feeding the antenna system so that the radiated electromagnetic wave will have a 90° phase difference between y component (E_y) and x component (E_x). In the case of generating left-hand circular polarization (LHCP) the value of δ equals to -90° and for right-hand circular polarization (RHCP) the value of δ equals to 90°.

2.2 LP-SAR System

In the conventional LP-SAR system, the 3-dB (half power) beamwidth of the antenna is used to determine some basic parameters. In the elevation/range direction, the 3-dB beamwidth ($\theta_{el\text{-}LP}$) will determine the swath width ground that could be covered by the system. On the other hand, at the azmituh direction, the 3-dB beamwidth ($\theta_{az\text{-}LP}$) is related to the synthetic aperture length (L_{sa}), for instance, which can be found as (Tomiyasu, 1978)

$$L_{sa} = R_o \theta_{az-LP} \tag{2}$$

where L_{sa} = the length of synthetic aperture
R_o= the nearest range distance to the target in azimuth plane view (described in figure 5.b)

Both of these half power beamwidth are immediately determined by the physical size of antenna as (Stimson, 1998) as

$$\theta_{el-LP} = \frac{\lambda}{W}$$
$$\theta_{az-LP} = \frac{\lambda}{L} \tag{3}$$

where W = physical antenna width
L = physical antenna length
λ = radar wavelength

2.3 CP-SAR System

Different from LP-SAR system, in our novel CP-SAR system the applied antenna beamwidth is more determined by the AR characteristic of the antenna rather than only the physical size of the antenna. Here, within the targeted beamwidth, the antenna should have AR ≤ 3dB. Although theoretically perfect circularly polarized wave is achieved when AR is 0 dB, our experiment results (Baharuddin et al., 2009 and 2010; Sri Sumantyo et al., 2005) shows that it is practically very difficult to be realized. Hence, we defined our 3-dB AR beamwidth parameter as

$$\theta_{el-CP} \le 3-dB\ AR\ and\ \theta_{el-LP}$$
$$\theta_{az-CP} \le 3-dB\ AR\ and\ \theta_{az-LP} \tag{4}$$

where $\theta_{el\text{-}CP}$ = 3-dB AR beamwidth in elevation direction
$\theta_{az\text{-}CP}$ = 3-dB AR beamwidth in azimuth direction

Both $\theta_{el\text{-}LP}$ and $\theta_{az\text{-}LP}$ are explained in equation (3). Figure 3 gives us explanation about this 3-dB AR limitation.

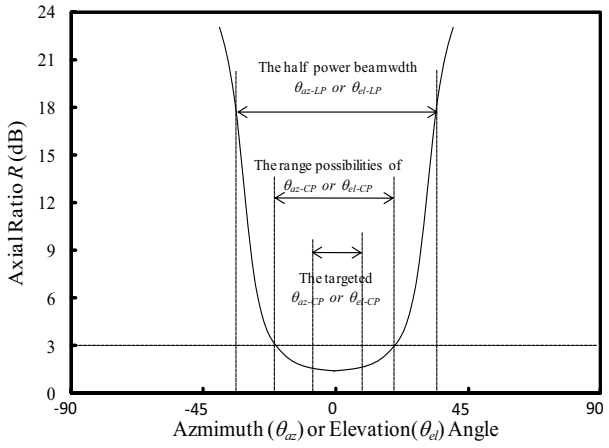

Figure 3. The 3-dB AR beamwidth illustration

3. UAV CP-SAR DESIGN

3.1 UAV CP-SAR Sensor Hardware Design

In general, the hardware of UAV CP-SAR sensor can be divided into two main systems which are antenna system and circuit system (figure 4). In the antenna system part, an antenna system having simultaneous RHCP and LHCP transmission and reception are developed with direct feeding method. The circuit system part consists of two subsystems which are transmitter and receiver subsystem. Filter components, such as low pass filter (LPF) and band pass filter (BPF) are implemented in both subsystems to assure only the wanted radar signal is processed. In the transmitter, the chirp signal is shifted to the RF frequency (1.27 GHZ as the center frequency) by using up-converter mixer and then amplified by high power amplifier (HPA) to obtain adequate power transmit in the system. In the receiver part, firstly, the reflected signal is amplified by Low Noise Amplifier (LNA) and then shifted to the baseband frequency by using down-converter mixer hence the received signal is ready to be sampled and digitized by analog to digital converter (ADC) unit. The clock unit controls and manages the timing for many components in the sensor such as the chirp generator, the signal processor component and also the frequency generator. This timing function is correlated to transmitting and receiving timing of the chirp pulse.

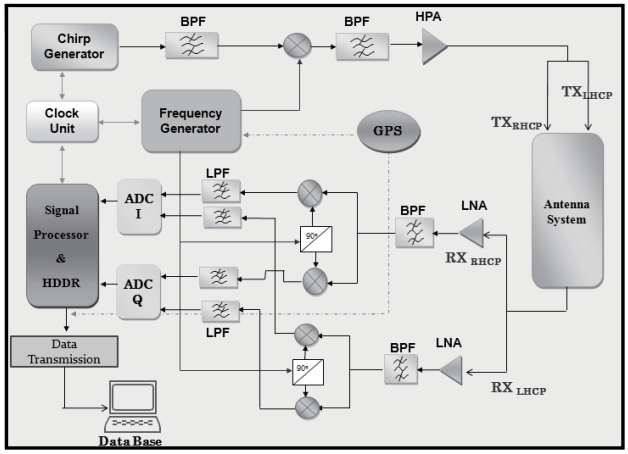

Figure 4. UAV CP-SAR sensor circuit design

3.2 UAV CP-SAR Parameter Design

Figure 5 illustrate the CP-SAR geometry system both in slant range and azimuth view. Here, H is the airborne altitude, θ_o is off nadir angle, θ_i is incidence angle, W_g is the desired swath width and $W_{g\ max}$ is the maximum swath width. Parameter R_m is the CP-SAR middle slant range, R_a (R_n) is CP-SAR near slant range, R_b (R_f) is CP-SAR far slant range for the desired swath width (maximum swath width). In our CP-SAR system, the slant range parameters will be depend on the value of $\theta_{el\text{-}CP}$ as shown in the following equation

$$R_n = \frac{H}{\cos\left(\theta_o - \left(\theta_{el-CP}/2\right)\right)} \tag{5}$$

$$R_m = \frac{H}{\cos\theta_o}$$

$$R_f = \frac{H}{\cos\left(\theta_o + \left(\theta_{el-CP}/2\right)\right)}$$

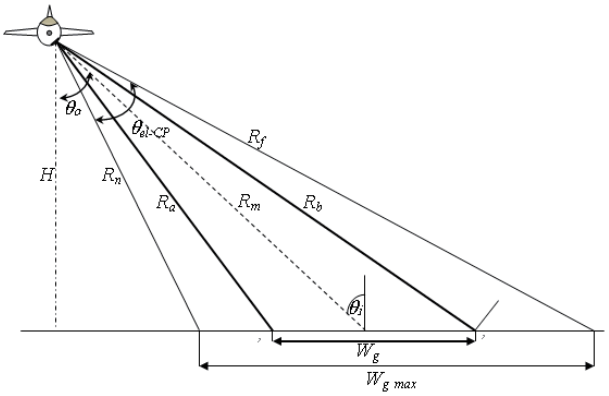

(a)

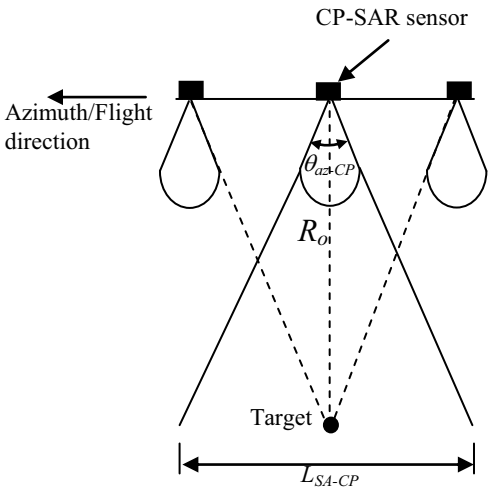

(b)

Figure 5. UAV CP-SAR geometry system: (a) slant range view and (b) azimuth plane view

If W_g is set to be equal with $W_{g\ max}$, then $R_a = R_n$ and $R_b = R_f$. The required $\theta_{el\text{-}CP}$ to obtain the desired swath width can be estimated by solving equation (6) below

$$W_g = \sqrt{R_f^{\,2} - H^2} - \sqrt{R_n^{\,2} - H^2} \tag{6}$$

$$\sqrt{\left(\frac{1}{\cos\left(\theta_o + \left(\theta_{el-CP}/2\right)\right)}\right)^2 - 1} - \sqrt{\left(\frac{1}{\cos\left(\theta_o - \left(\theta_{el-CP}/2\right)\right)}\right)^2 - 1} - \frac{W_g}{H} = 0$$

The CP-SAR azimuth resolution, $\delta_{az\text{-}CP}$, can be calculated as

$$L_{SA-CP} = R_o \theta_{az-CP}$$
$$\delta_{az-CP} = \frac{R_o \lambda}{2L_{SA-CP}} = \frac{\lambda}{2\theta_{az-CP}} \quad (7)$$

where L_{sa} = the length of synthetic aperture of CP-SAR

From equation (7) above can be found that the azimuth resolution in the CP-SAR system depends on $\theta_{az\text{-}CP}$ rather than the length of physical antenna size.

In the range direction the gorund range resolution, $\delta_{rg\text{-}CP}$, is determined by the transmitted chirp bandwidth and the incidence angle as can be expressed in

$$\delta_{rg-CP} = \frac{c}{2B \sin \theta_i} \quad (8)$$

where c = light velocity ($3x10^8$ ms^{-1})
B = chirp pulse bandwidth

The incidence angle θ_i can be estimated using the following equation:

$$\theta_i = \sin^{-1}\left(\sin \theta_o \frac{R_e + H}{R_e} \right) \quad (9)$$

where R_e = Earth radius (≈ 6371 km)

In the case of airborne system, the value of H is relative small compare to R_e ($H << R_e$) hence the result of $\theta_i \approx \theta_o$ will be obtained.

The other basic parameters, such as the required transmitted peak power (P_t) and the required flight time to obtain data image (t_D) can be estimated using equation

$$SNR = \frac{P_t (G\eta)^2 \lambda^3 (PRF) \sigma^\circ c \tau_p}{(4\pi)^3 R^3 KTBF 4vL_s \sin \theta_i} \quad (10)$$

where SNR = signal to noise ratio
G = antenna gain
η = antenna effeciency
PRF = pulse repetition frequency
σ° = the value of backscattering coefficient
τ_p = the transmitted pulse length
R = radar slant range
K = Boltzman coefficient ($1.38x10^{-23}$ JK^{-1})
T = receiver temperature (in Kelvin)
F = receiver noise figure
v = UAV velocity
L_s = system loss

$$t_D = \frac{L}{v}$$
$$L = Y_o + L_{sa} \quad (11)$$

where Y_0 = the length of image size

4. UAV CP-SAR PARAMETERS CALCULATION RESULTS

In our design, it is targeted that the value of resolution has relationship with the swath witdth W_g as

$$\delta_{rg-CP} = \frac{W_g}{1000}$$
$$\delta_{az-CP} = \delta_{rg-CP} \quad (12)$$

Here, cell resolution equals to around 1 m is targeted. Hence, based on equation (12), the desired W_g should be around 1 km. In order to obtain this W_g, equation (4) and (6) is used to determine the required $\theta_{el\text{-}CP}$. Since the $\delta_{az\text{-}CP}$ is also set to 1 m (equation (12)), then the required $\theta_{az\text{-}CP}$ can also be estimated using equation (7). Figure 6 shows the list of the required $\theta_{el\text{-}CP}$ and $\theta_{az\text{-}CP}$, for operational θ_o from 40° up to 60°. Here, equation (3) would give maximum value of $\theta_{el\text{-}CP}$ and $\theta_{az\text{-}CP}$. Employing 1.5m x 0.4 m antenna size in our CP-SAR sensor, maximum value of $\theta_{el\text{-}CP}$ and $\theta_{az\text{-}cP}$ equal to 29.78° and 7.94°.From figure 6 can be found that smaller $\theta_{el\text{-}CP}$ for higher altitude and almost constant $\theta_{az\text{-}CP}$ will be required. In figure 6.a, for θ_o equals to 40° and 41°, the maximum W_g that could be obtained are around 0.95 and 0.99 km due to half power beam width limitation in equation (3). Hence the targeted resolution becomes 0.95 and 0.99 m (equation 12). This situation makes a small not constant curve in figure 6.b.

In our CP-SAR system, the image data that received in the range direction, will be sampled and process during the receiving window period (T_{rw}). This T_{rw} is defined as

$$T_{rw} = t_{\max} - t_n$$
$$t_n = 2R_n / c$$
$$t_{\max} = 2R_{\max} / c + \tau_p$$
$$R_{\max} = \sqrt{R_f^2 + \left(L_{sa}/2 \right)^2} \quad (13)$$

where t_n = range sampling start time
t_{max} = range sampling stop time

Here, a high accurate timing in sampling process (precise start (t_n) and stop time (t_{max})) is required in order to processed image data that captured only by $\theta_{el\text{-}CP}$ which based on equation (5) determines the R_n and R_f parameters in equation (13).

In azimuth direction, the processed Doppler bandwidth (B_p) will ensure only data that capture by $\theta_{az\text{-}CP}$ is handled. This situation

can be seen applying $\theta_{az\text{-}CP}$ parameters in the following equations (Curlander and McDonough., 1991; Stimson, 1989)

$$B_p \approx B_D$$
$$B_D \cong \frac{2v\theta_{az-CP}}{\lambda} \quad (14)$$

where B_D = Doppler bandwidth

From the above explanation can be obtained that the 3-dB AR beamwidth, both $\theta_{el\text{-}CP}$ and $\theta_{el\text{-}CP,}$ are become the main constraint in our hardware, parameter and signal processing design. This situation give us the possibility to realize a smaller SAR sensor, especially in the antenna size, since some CP-SAR basic parameters such as the targeted W_g and $\delta_{az\text{-}CP}$ are determined by the 3-dB AR antenna beamwidth ($\theta_{el\text{-}CP}$ and $\theta_{el\text{-}CP}$) and not immediately determined by the physical size of antenna anymore.

The required B and P_t are plotted in figure 7 based on equations (8) up to (10). Higher transmitted peak power is required for higher platform altitude and narrower chirp pulse bandwidth can be applied when higher θ_o is used. The summary of our UAV CP-SAR parameters are shown in table 2.

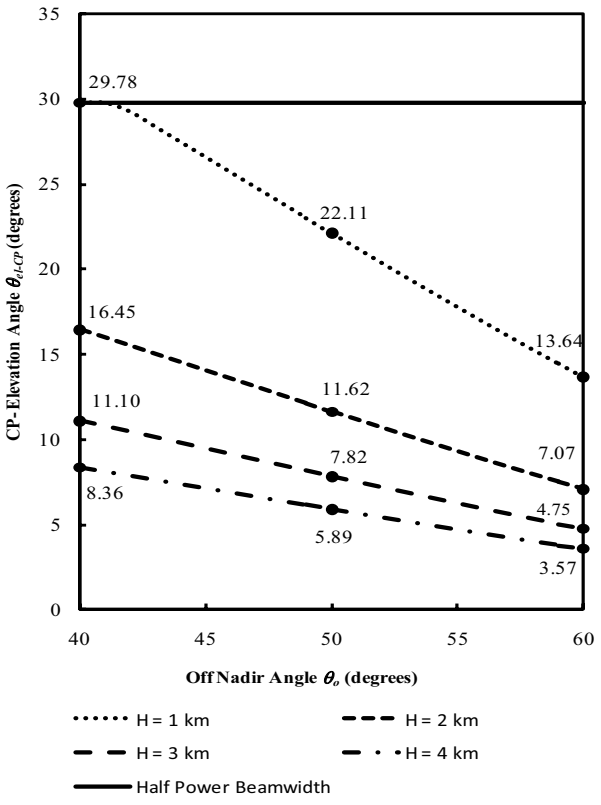

(a)

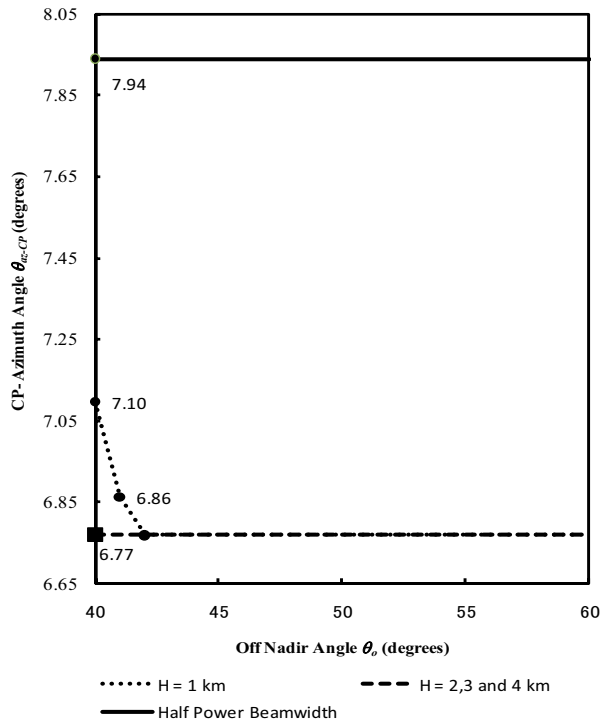

(b)

Figure 6. The required (a) $\theta_{el\text{-}CP}$ and (b) $\theta_{az\text{-}CP}$ for 1 m image resolution

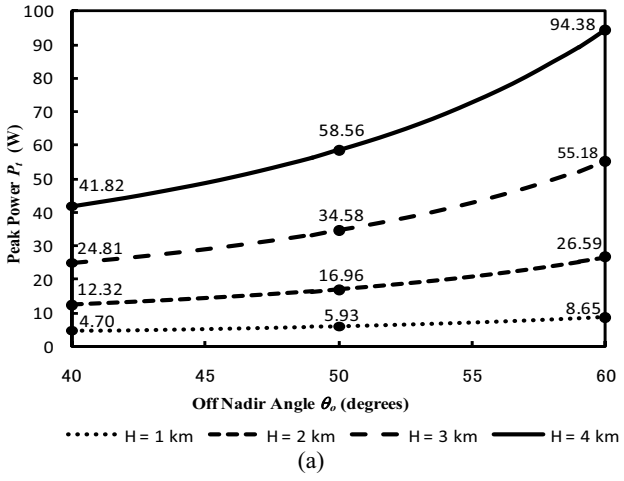

(a)

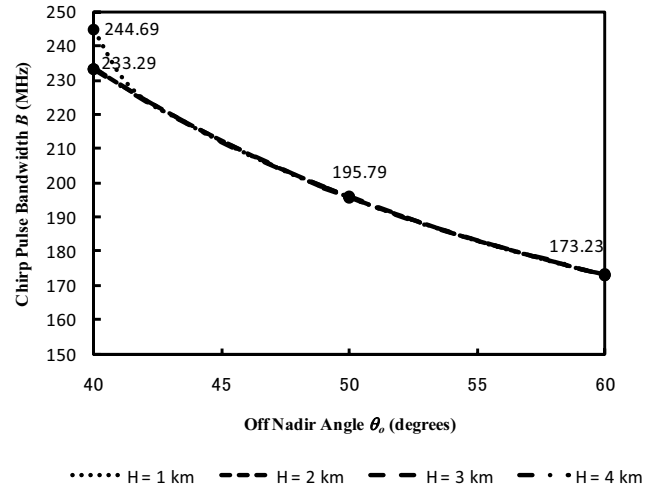

(b)

Figure 7. The required (a) P_t and (b) B for 1 m image resolution

Parameter	Specification
Altitude	1 – 4 km
Frequency	1.27 GHz (L-Band)
Polarization	**Tx : RHCP + LHCP** **Rx : RHCP + LHCP**
Image Size	50 km^2
Pulse Length	3.9 up to 23.87 μs
Pulse Bandwidth	61.14 up to 244.69 MHz
Off Nadir	40° up to 60°
Resolution	≈1m
Swadth width	1 km
Antenna Size	1.5 m x 0.4 m
Azimuth Beamwidth	6.77°-7.1°
Elevation Beamwidth	3.57°-29.78°
Axial Ratio	**≤3 dB**
Antenna Efficiency	60%
PRF	1000 Hz
Peak Power	8.65 W up to 94.38 W (4 km)
Average Power	20.59 mW up to 4.5 W
System :	
Noise Figure	3 dB
Temperature	500 K
Loses System	7 dB
Switching Time	3 μs
SNR	15 dB
Data Take Duration	≈31.70 minutes

Table 2. UAV CP –SAR Specification

5. CONCLUSSION

In this paper, the definition of a novel CP-SAR system has already explained. The 3-dB AR beamwidth in both elevation and azimuth of the antenna are became the main constraint in the hardware, parameter and signal processing design. This 3-dB AR dependency make a small sensor is possible to be implemented in the CP-SAR system. Furthermore, this research will be a remarkable point to the CP-SAR sensor onboard a small satellite realization in the future.

REFERENCES

Baharuddin, M., Wissan,V., Tetuko S.S, J. and Kuze,H., 2009. Equilateral triangular microstrip antenna for circularly-polarized synthetic aperture radar. *Journal of Progress in Electromagnetic Research C*, 8, pp. 107-120.

Baharuddin, M., Rizki Akbar, P., Tetuko S.S, J., and Kuze, H., 2010. Development of circularly polarized synthetic aperture radar sensor mounted on unmanned aerial vehicle. *Jurnal Otomasi, Kontrol & Instrumentasi (Journal of Automation, Control and Instrumentation)*, 1, pp. 1-6.

Curlander, J.C and McDonough, R.N, 1991. *Synthetic Aperture Radar Systems and Signal Processing*, Wiley, USA.

Dubois-Fernandez, P.C., Souyris, J.-C; Angelliaume, S., Garestier, F., 2008. The compact polarimetry alternative for spaceborne SAR at low frequency. *IEEE Transactions on Geoscience and Remote Sensing*, 46, pp. 3208-3222.

Freeman, A., 2003. Faraday Rotation and Interferometric/Polarimetric SAR. http://trs-new.jpl.nasa.gov/dspace/bitstream/2014/7609/1/03-1625.pdf (accessed 11 May 2010).

ITU, 2002. Handbook on Satellite Communications, 3rd edn. Wiley, USA, pp. 96-97.

Meyer, F.J. and Nicoll, J.B., 2008. Prediction, detection, and correction of Faraday rotation in full-polarimetric L-band SAR data. *IEEE Transaction on Geoscience and Remote Sensing*, 46, pp. 3076-3086.

Raney, R.K., 2007, Hybrid-polarity SAR architecture. *IEEE Transactions on Geoscience and Remote Sensing*, 45, pp. 3397-3404.

Rignot, E.J.M., 2000. Effect of Faraday rotation on L-band interferometric and polarimetric synthetic-aperture radar data. *IEEE Transactions on Geoscience and Remote Sensing*, 38, pp. 383-390.

Rizki Akbar, P., Tetuko S. S, J. and Kuze, H., 2010. A novel circularly polarized synthetic aperture radar (CP-SAR) onboard spaceborne platform. *International Journal of Remote Sensing*, 31(04), pp. 1053 – 1060.

Sri Sumantyo, J.T., Ito, K. and Takahashi, M., 2005. Dual-band circularly polarized equilateral triangular-patch array antenna for mobile satellite communications. *IEEE Transaction Antennas and Propagation*, 53, pp. 3477-3485.

Sri Sumantyo,J.T., Wakabayashi, H., Iwasaki, A., Takahashi, F., Ohmae, H., Watanabe, H., Tateishi, R., Nishio, F., Baharuddin, M., and Rizki Akbar, P., 2009. Development of circularly polarized synthetic aperture radar onboard microsatellite. In: *Progress in Electromagnetics Research Symposium (PIERS-2009) Proceedings*, Beijing, China, pp. 382 – 385.

Stimson, G.W., 1989. *Introduction to Airborne Radar, 2nd edn.* SciTech Publishing Inc., USA, Chap.8.

Stutzman, W.L., 1993. *Polarization in Electromagnetic System*. Artech House, USA.

Tomiyasu, K. Tutorial review of Synthetic-Aperture Radar (SAR) with applications to imaging of the ocean surface. In: *Proceedings of the IEEE*, 66, pp. 563-583.

Wright, P.A.; Quegan, S.; Wheadon, N.S.; Hall, C.D., 2003. Faraday rotation effects on L-band spaceborne SAR data, *IEEE Transactions on Geoscience and Remote Sensing,* 41, pp. 2735-2744.

ACKNOWLEDGEMENTS

The authors would like to thank the Japan Society for the Promotion of Science (JSPS) for Grant-in-Aid for Scientific Research 2007-Young Scientist (A) (No. 19686025) and National Institute of Information and Communication Technology (NICT) for International Research Collaboration Research Grant.